



Near-infrared induced optical quenching effects on mid-infrared quantum cascade lasers

Dingkai Guo, Hong Cai, Muhammad Anisuzzaman Talukder, Xing Chen, Anthony M. Johnson, Jacob B. Khurgin, and Fow-Sen Choa

Citation: *Applied Physics Letters* **104**, 251102 (2014); doi: 10.1063/1.4884605

View online: <http://dx.doi.org/10.1063/1.4884605>

View Table of Contents: <http://scitation.aip.org/content/aip/journal/apl/104/25?ver=pdfcov>

Published by the [AIP Publishing](#)

Articles you may be interested in

[Femtosecond measurements of near-infrared pulse induced mid-infrared transmission modulation of quantum cascade lasers](#)

Appl. Phys. Lett. **104**, 211101 (2014); 10.1063/1.4880358

[Dispersion of effective refractive indices of mid-infrared quantum cascade lasers](#)

J. Appl. Phys. **112**, 103109 (2012); 10.1063/1.4766388

[Importance of interface roughness induced intersubband scattering in mid-infrared quantum cascade lasers](#)

Appl. Phys. Lett. **101**, 171117 (2012); 10.1063/1.4764516


[Wall-plug efficiency of mid-infrared quantum cascade lasers](#)

J. Appl. Phys. **111**, 053111 (2012); 10.1063/1.3692392

[Coherent near-infrared wavelength conversion in semiconductor quantum cascade lasers](#)


Appl. Phys. Lett. **89**, 183507 (2006); 10.1063/1.2374842

Agilent's Electronic Measurement Group is becoming **Keysight Technologies**.



Engineering Education & Research Resources DVD 2014

Agilent is the key to your test and measurement needs **Order yours**



Agilent Technologies

The advertisement features a red header with the text 'Agilent's Electronic Measurement Group is becoming Keysight Technologies.' Below this is a row of ten icons representing various engineering and research fields: a Wi-Fi symbol, a checkmark, a graduation cap, an open book, a sun, a network diagram, a radio tower, a microchip, a sine wave, a vertical bar chart, and a starburst. The central focus is a DVD cover for 'Agilent Technologies Engineering Education & Research Resources DVD 2014'. The cover is blue and white with a grid of small icons. Below the DVD cover, the text 'Engineering Education & Research Resources DVD 2014' is written in a bold, black font. Underneath that, the slogan 'Agilent is the key to your test and measurement needs' is followed by a red button with the text 'Order yours'. At the bottom, the Agilent Technologies logo (a starburst) and the company name 'Agilent Technologies' are displayed on a blue background.

Near-infrared induced optical quenching effects on mid-infrared quantum cascade lasers

Dingkai Guo,^{1(a)} Hong Cai,² Muhammad Anisuzzaman Talukder,¹ Xing Chen,¹ Anthony M. Johnson,^{1,2} Jacob B. Khurgin,³ and Fow-Sen Choa^{1,2}

¹Department of Computer Science and Electrical Engineering, University of Maryland, Baltimore County, 1000 Hilltop Circle, Baltimore, Maryland 21250, USA

²Center of Advanced Studies in Photonics Research (CASPR), University of Maryland, Baltimore County, 1000 Hilltop Circle, Baltimore, Maryland 21250, USA

³Department of Electrical and Computer Engineering, Johns Hopkins University, Baltimore, Maryland 21218, USA

(Received 5 May 2014; accepted 10 June 2014; published online 23 June 2014)

In space communications, atmospheric absorption and Rayleigh scattering are the dominant channel impairments. Transmission using mid-infrared (MIR) wavelengths offers the benefits of lower loss and less scintillation effects. In this work, we report the telecom wavelengths (1.55 μm and 1.3 μm) induced optical quenching effects on MIR quantum cascade lasers (QCLs), when QCLs are operated well above their thresholds. The QCL output power can be near 100% quenched using 20 mW of near-infrared (NIR) power, and the quenching effect depends on the input NIR intensity as well as wavelength. Time resolved measurement was conducted to explore the quenching mechanism. The measured recovery time is around 14 ns, which indicates that NIR generated electron-hole pairs may play a key role in the quenching process. The photocarrier created local field and band bending can effectively deteriorate the dipole transition matrix element and quench the QCL. As a result, MIR QCLs can be used as an optical modulator and switch controlled by NIR lasers. They can also be used as “converters” to convert telecom optical signals into MIR optical signals. © 2014 AIP Publishing LLC. [<http://dx.doi.org/10.1063/1.4884605>]

Mid-infrared (MIR) sources within the air windows (3–5 and 8–12 μm) have great potential to be used for both space communications and free-space optical communications (FSOC) due to their lower Mie and Rayleigh scattering losses, better scintillation performance, higher modulation bandwidth, and better eye-safe compatibility compared to near-infrared (NIR) sources.^{1–3} NIR optical communications are mature technologies. Current commercial FSOC systems are primarily based on the adaptation of telecom components in the NIR spectral region. The ability to convert NIR signal to MIR signals will be highly desirable for many future applications.

Near-infrared interactions with mid-infrared quantum cascade lasers (QCLs) have been reported previously. Using a 750 nm NIR source to inject into an open window on the QCL ridge, Zervos *et al.* observed threshold reduction, output power enhancement, and up to 100% all optical modulation near threshold at very low or DC operation speed.⁴ Using a 820 nm Ti:sapphire laser to inject into QCL waveguide, Chen *et al.* observed fast (81 ps) optical quenching with 18% modulation depth,⁵ and fast MIR wavelength modulation (up to 1.67 GHz).⁶ In this work, we report near 100% modulation of MIR QCLs using telecom wavelengths (1.55 μm and 1.3 μm) induced optical quenching effects when QCLs are biased well above threshold. There have also been prior works on interaction between the near and mid- (or far-) infrared in quantum wells.^{7,8} While in those works the multi-quantum-wells (MQWs) were passive or served as a nonlinear mixer, the MQW medium in our device is active.

Furthermore, while the interactions in Ref 7 were coherent (i.e., dependent on relative phase of two waves), the interactions in our work are not phase-dependent.

All experiments described in the following were carried out on a group of strain-compensated InGaAs/InAlAs QCLs with emitting wavelengths around 4.8 μm . The structure was grown by metalorganic chemical vapor deposition (MOCVD) on an n-type InP substrate ($n = 2 \times 10^{17} \text{cm}^{-3}$). The active region is about 3 μm thick and is sandwiched by 0.5 μm thick InGaAs layers on both the bottom and top sides. The active region structure is similar to the one published in Ref. 9. The cap InP layers include a 2.5 μm thick of low doped ($1 \times 10^{17} \text{cm}^{-3}$) upper waveguide cladding layer, a 1 μm of thick high doped ($1 \times 10^{19} \text{cm}^{-3}$) plasmon-enhanced confinement layer, and a 100 Å of heavily doped ($>10^{19} \text{cm}^{-3}$) contact layer. After the cover growth, the sample was processed with a standard buried-heterostructure (BH) regrowth to form the 12 μm waveguide structure with both photonic and electronic confinements.¹⁰ Ti/Au was used for both top and bottom metallization. The samples were then cleaved and scribed down to 3 mm long and 0.5 mm wide devices and mounted epi-side down on copper heat sinks. Both ends of the QCLs were uncoated.

The first part of the experiment has a setup as shown in Figure 1(a). A 1550 nm tunable diode laser plus an Er-doped amplifier were used as the near-infrared source. The chopped NIR lights were collimated and focused onto the QCL front facet and well coupled into the QCL waveguide. After the coupling was optimized by using methods described in Ref. 11, both the NIR and MIR laser beams from the other end of the QCL were collimated by a ZnSe lens and sent into

^{a)}Author to whom correspondence should be addressed. Electronic mail: dingk1@umbc.edu

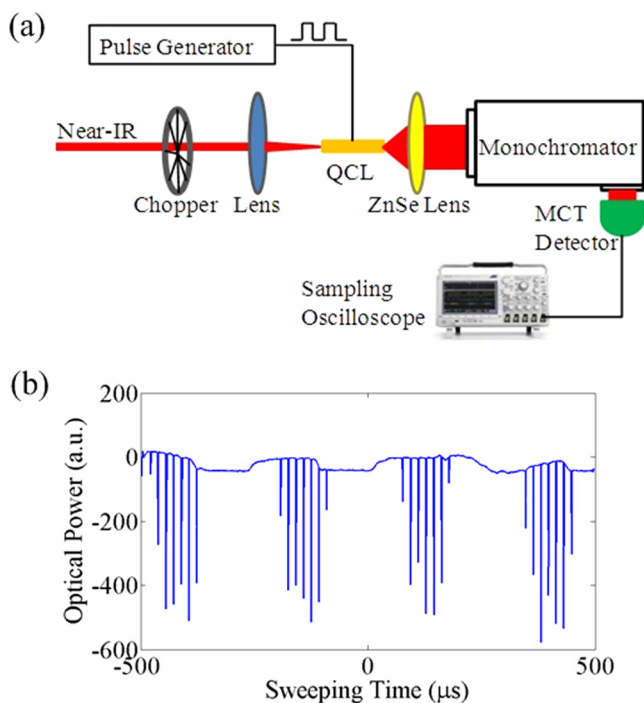


FIG. 1. (a) The setup for telecom wavelengths induced quenching effects on mid-infrared QCLs. (b) The screenshot of the sampling oscilloscope: the mid-infrared pulse train detected with the MCT detector (negative voltage output) as a function of the modulated near-infrared input and the oscilloscope sweeping time.

a monochromator, which functions as an optical filter to separate the two wavelengths. A photovoltaic mercury cadmium telluride (MCT) detector by Vigo System S.A. with a four-stage TE cooler is used at the monochromator output to measure the filtered MIR QCL light intensity.

In the experiments, the mid-infrared QCL was under pulse-mode operations. A pulse generator was used to drive the QCL with electrical pulse duration of 110 ns and amplitude of ~ 9.8 V. We modulated the NIR pump source using a chopper at a frequency from 1 kHz to 10 kHz and observed the MIR output on an oscilloscope. Figure 1(b) is a screenshot of the oscilloscope showing the observed QCL output, as a pulse train determined by the repetition rate of the electrical driving pulses. A slower modulation envelope produced by the chopper was shown on top of the pulse train. The base line fluctuation was caused by the scattering of the NIR light inside the monochromator and picked up by the MCT detector. This was verified by reducing the NIR power and observing the diminution of the baseline modulation. It was observed that when the 1550 nm light was blocked by the chopper, the MIR pulse train showed up; when the NIR light was unblocked and well coupled into the QCL waveguide, the MIR pulse train was quenched.

Then we gradually increased the NIR input power into the MIR waveguide and looked at the MIR output with the MCT detector. By varying the NIR laser power from 0 mW to 20 mW, the corresponding MIR output is shown in Figure 2. When the NIR pump power is increased, the MIR laser output quickly drops initially. It then slowly drops down and approaches to zero when the pump power reaches 20 mW.

The quenching effect also depends on the coupled NIR wavelength. The NIR diode laser power was then fixed at

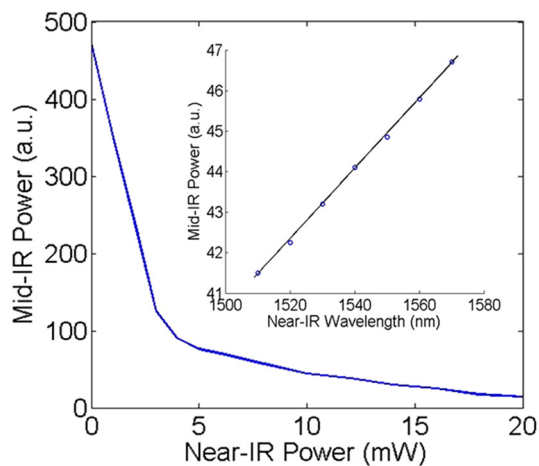


FIG. 2. The mid-infrared power amplitude as a function of the incident 1550 nm light power; Inset: The mid-infrared power vs. coupled near-infrared light wavelength.

2 mW, and its wavelength was tuned from 1510 nm to 1570 nm. The corresponding MIR light power from the QCL is recorded in the inset of Figure 2. It shows that the MIR QCL optical power amplitude has a roughly linear dependence on the NIR pump laser wavelength in this wavelength range. The coupling efficiency of shorter NIR photons into the MIR waveguide is higher may due to the fact that their absorption quantum efficiency near the bandtail is higher.

To explore the quenching mechanism, we conducted a time-resolved experiment by coupling ~ 1.3 μm , femtosecond pulses into the QCL waveguide. A Ti:Sapphire laser pumped optical parametric amplifier system¹² was used to provide fs pulses, which have a < 160 fs duration and a 250 kHz repetition rate. The QCL was running in pulsed mode, driven by 200 ns duration electrical pulses, and synchronized with the 1.3 μm pulses at 250 kHz repetition rate. The MIR output of the QCL was measured by a fast MCT detector and a sampling oscilloscope. Long pass filters were inserted in front of the MCT detector to only pass MIR signals and remove NIR signals. Figure 3(a) shows the electrical driving signal sent to the QCL. With certain time delays the QCL turns on and off with a time shift and also with a sharper rising and fall times as shown in Figure 3(b). Figure 3(b) shows MCT detector outputs with (red line) and without (black line) the ultrafast ~ 1.3 μm pulse pumping into the QCL. Figure 3(c) shows the time response of the MCT detector calibrated directly using the ~ 1.3 μm fs pulse. The corresponding full pulse duration is ~ 9 ns with a falling edge time constant around 4 ns. In the quenching process as shown in Figure 3(b), the MIR output drop 85% in 4 ns, which may be detector limited. It takes additional 12.4 ns to go down to the minimum close to zero. In the recovery process, it takes around 14 ns for the MIR signal to fully recover from the minimum point to its original level.

From the measured results, we would like to identify possible quenching processes. Since the measured relaxation times are mostly in the tens of nanoseconds range, the quenching mechanism is related to carrier dynamics of the photo-generated electron-hole pairs. Due to the higher effective mass of the holes, some of the holes might be trapped in the valance band hetero-structures and mostly trapped in the active region right against each injection barrier due to its

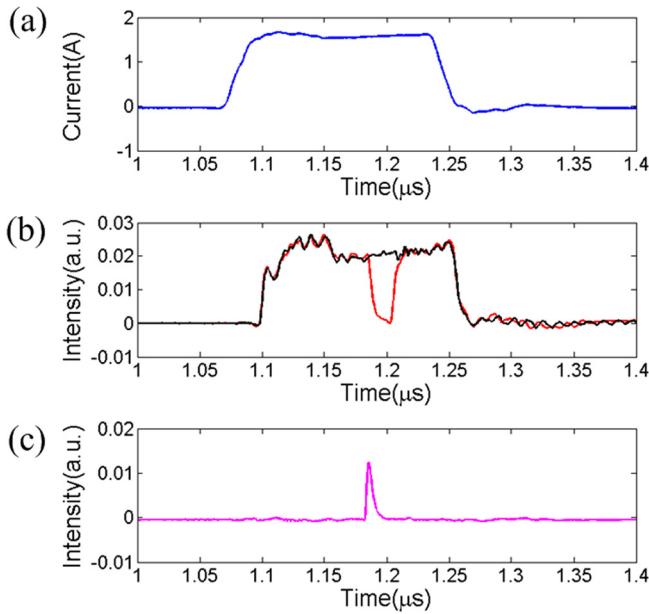


FIG. 3. The mid-infrared quenching speed measurement by coupling the ultrashort (<160 fs) $1.3 \mu\text{m}$ pulses into the QCL waveguide and measuring the QCL output. The QCL and ultrashort pulses were synchronized at 250 kHz. (a) The measured QCL current pulse. (b) QCL MIR output without (black line) and with (red line) the ultrashort pumping signal. (c) The response of a near-infrared fs pulse on the MCT detector. The detector speed limited measurement shows a pulse duration ~ 9 ns with ~ 4 ns fall time (90%–10%).

thick InAlAs layer; while the electrons, being mobile, will be distributed more or less evenly. The space charge field can create the potential as shown in the Figure 4. One can estimate the value of the amplitude of this potential as

$$V \sim \frac{e d^2}{\epsilon} n_p, \quad (1)$$

where d is the period of superlattice and n_p is the density of photo-generated holes. And

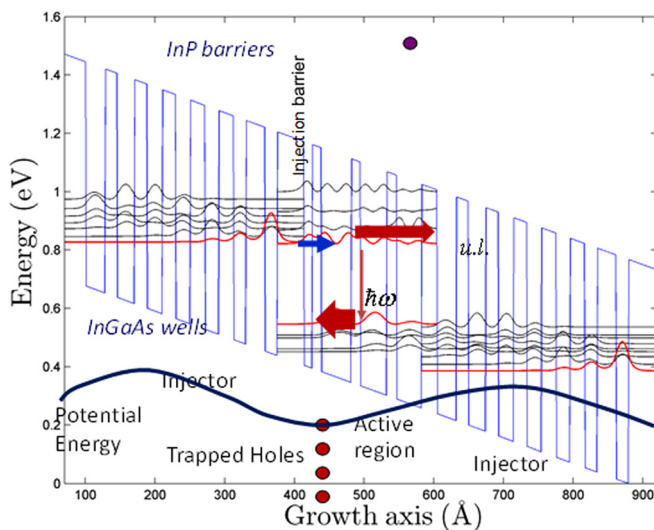


FIG. 4. The near-infrared induced hole-trapping and local electrical field in the mid-infrared quantum cascade lasers. Most of the trapped holes generated by the NIR illumination are trapped in the active region right against the tunneling barrier (shown as the big red arrow) and electrons are spread over (shown with the small red arrow). The created local field is opposite to the applied bias field and will provide a potential (blue curve) and band bending to quickly deteriorate the dipole matrix element and quench the QCL output.

$$n_p = \frac{\alpha P \tau_p}{A h \nu}, \quad (2)$$

where τ_p is the recombination time, P is the coupled optical power, A is the illuminated area, and α is absorption coefficient. So we obtain

$$V \sim \frac{e}{h \nu \epsilon} \frac{\alpha d^2 P \tau_p}{2A}. \quad (3)$$

By assuming a waveguide coupling efficiency of 10%, an absorption coefficient of $5 \times 10^4 \text{ cm}^{-1}$ and that all the photo-generated holes are trapped at one end of each active region, the estimation shows that only 1 mW of $1.3 \mu\text{m}$ near-infrared input can induce 1.6 V of band bending for one period of the QCL structure, which can effectively quench the QCL as described in the following. With the photo-generated space charge field, the states in the injector will go out of alignment and the tunneling resonance will be disturbed. More importantly, in the active region as shown in Figure 4, the lower laser state will be pushed left, attracted by the holes, and the upper laser state will be thrown right in order to maintain orthogonality with the lower state. The dipole matrix element, Z^2 , will deteriorate dramatically. As a result, nonradiative decay will quickly dominate the process and the MIR lasing will be quenched. With such an understanding, we realize that the NIR wavelength dependence of quenching may simply be caused by wavelength dependent NIR absorptions of QCL cavity.

In conclusion, near-infrared signals coupled into mid-infrared QCL waveguide can simultaneously change the device electrical conductance and the MIR light output. The change depends on NIR light power, wavelength, and MIR QCL structure. We experimentally studied the phenomenon with telecom wavelength pump lasers and $4.8 \mu\text{m}$ QCLs. This technique has the potential to be used for direct optical conversion of telecom signals into MIR signals.

This work was supported by MIRTHE (NSF-ERC) and the authors thank Robert J. Weiblen for helpful discussions.

- ¹R. Martini, C. Gmachl, J. Falciglia, F. G. Curti, C. G. Bethea, F. Capasso, E. A. Whittaker, R. Paiella, A. Tredicucci, A. L. Hutchinson, D. L. Sivco, and A. Y. Cho, *Electron. Lett.* **37**(3), 191–193 (2001).
- ²A. Soibel, M. W. Wright, W. H. Farr, S. A. Keo, C. J. Hill, R. Q. Yang, and H. C. Liu, *IEEE Photon. Technol. Lett.* **22**(2), 121–123 (2010).
- ³R. Martini and E. A. Whittaker, *J. Opt. Fiber. Commun. Rep.* **2**, 279–292 (2005).
- ⁴C. Zervos, M. D. Frogley, and C. C. Phillips, *Appl. Phys. Lett.* **90**, 053505 (2007).
- ⁵G. Chen, C. G. Bethea, R. Martini, P. D. Grant, R. Dudek, and H. C. Liu, *Appl. Phys. Lett.* **95**, 101104 (2009).
- ⁶G. Chen, R. Martini, S.-W. Park, C. G. Bethea, I. A. Chen, P. D. Grant, R. Dudek, and H. C. Liu, *Appl. Phys. Lett.* **97**, 011102, (2010).
- ⁷B. Zaks, H. Banks, and M. S. Sherwin, *Appl. Phys. Lett.* **102**, 012104 (2013).
- ⁸C. Phillips, M. Y. Su, M. S. Sherwin, J. Ko, and L. Coldren, *Appl. Phys. Lett.* **75**, 2728 (1999).
- ⁹X. J. Wang, J. Y. Fan, T. Tanbun-Ek, and F.-S. Choa, *Appl. Phys. Lett.* **90**, 211103 (2007).
- ¹⁰L. Cheng, J. Fan, D. Janssen, D. Guo, X. Chen, F. J. Towner, and F.-S. Choa, *J. Electron. Mater.* **41**, 506–513 (2012).
- ¹¹D. Shyu, F.-S. Choa, X. Chen, and S. Trivedi, *Proc. SPIE* **7953**, 79531T (2011).
- ¹²S. Liu, E. Lalanne, P. Q. Liu, X. Wang, C. F. Gmachl, and A. M. Johnson, *IEEE J. Sel. Top. Quantum Electron.* **18**, 92–104 (2012).